Article

Stability of Thin-Film Solid-State Electroluminescent Devices Based on Tris(2,2‘-bipyridine)ruthenium(II) Complexes

Gregory Kalyuzhny, Mihai Buda, Jason McNeill, Paul Barbara, and Allen J. Bard

J. Am. Chem. Soc., **2003**, 125 (20), 6272-6283• DOI: 10.1021/ja029550i • Publication Date (Web): 26 April 2003

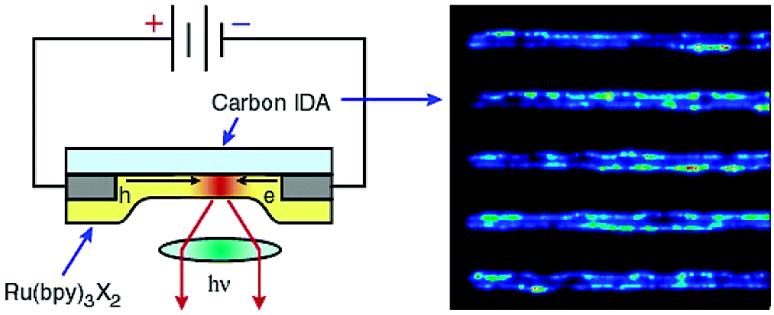

More About This Article

Additional resources and features associated with this article are available within the HTML version:

- Supporting Information
- Links to the 23 articles that cite this article, as of the time of this article download
- Access to high resolution figures
- Links to articles and content related to this article
- Copyright permission to reproduce figures and/or text from this article

View the Full Text HTML

J|A|C|S
ARTICLES
Published on Web 04/26/2003

Stability of Thin-Film Solid-State Electroluminescent Devices Based on Tris(2,2′-bipyridine)ruthenium(II) Complexes

Gregory Kalyuzhny, Mihai Buda, Jason McNeill, Paul Barbara, and Allen J. Bard*

Contribution from the Department of Chemistry and Biochemistry and Center for Nano- and Molecular Science and Technology, The University of Texas at Austin, Austin, Texas 78712

Received December 2, 2002; E-mail: ajbard@mail.utexas.edu

Abstract: The factors affecting the operating life of the light-emitting electrochemical cells (LECs) based on films of tris(2,2′-bipyridine)ruthenium(II) both in sandwich (using an ITO anode and a Ga:Sn cathode) and planar (using interdigitated electrode arrays (IDAs)) configurations were investigated. Stability of these devices is greatly improved when they are produced and operated under drybox conditions. The proposed mechanism of the LEC degradation involves formation of a quencher in a small fraction of tris(2,2′-bipyridine)-ruthenium(II) film adjacent to the cathode, where light generation occurs, as follows from the observed electroluminescence profile in the LECs constructed on IDAs, showing that the charge injection in such devices is highly asymmetric, favoring hole injection. Bis(2,2′-bipyridine)diaquoruthenium(II) is presumed to be the quencher responsible for the device degradation. A microscopic study of photo- and electroluminescence profiles of planar light-emitting electrochemical cells was shown as a useful approach for studies of charge carrier injection into organic films.

Introduction

The limited operating life of organic light-emitting devices (OLEDs) is an important factor preventing their wide-scale commercial use in various display applications. There have been many research efforts aimed at understanding OLED light emission decay mechanisms.[1−11] However, most of these reliability studies were carried out for devices based on tris-(8-hydroxyquinoline)aluminum (Alq_3).[1,3,5−7,10,11] A special case of OLEDs, light-emitting electrochemical cells (LECs), is characterized by the presence of mobile ions in the solid organic emitting layer.[12−17] During device operation, migration of the ions leads to formation of the concentration gradient facilitating the injection of charge carriers at contact interfaces. The steep interfacial potential gradients result in a substantial decrease of device operating voltage to a value, in some cases, close to the optical band gap of an organic semiconductor.[14,15,18,19] Several LECs presented thus far have been based on thin films of polymers[12,13,20−22] or small molecules, in particular, 1,2-diimine complexes of Ru[23−33] and Os.[33,34] As for OLEDs in general, the low stability of LECs is the main obstacle preventing them from wide commercial use. However, to our knowledge, there have been no systematic studies of the light emission decay of LECs.

(1) Burrows, P. E.; Bulovic, V.; Forrest, S. R.; Sapochak, L. S.; McCarty, D. M.; Thompson, M. E. *Appl. Phys. Lett.* **1994**, *65*, 2922−2924.
(2) Hamada, Y.; Sano, T.; Shibata, K.; Kuroki, K. *Jpn. J. Appl. Phys., Part 2* **1995**, *34*, L824-L826.
(3) McElvain, J.; Antoniadis, H.; Hueschen, M. R.; Miller, J. N.; Roitman, D. M.; Sheats, J. R.; Moon, R. L. *J. Appl. Phys.* **1996**, *80*, 6002−6007.
(4) VanSlyke, S. A.; Chen, C. H.; Tang, C. W. *Appl. Phys. Lett.* **1996**, *69*, 2160−2162.
(5) Aziz, H.; Popovic, Z.; Tripp, C. P.; Hu, N. X.; Hor, A. M.; Xu, G. *Appl. Phys. Lett.* **1998**, *72*, 2642−2644.
(6) Aziz, H.; Popovic, Z.; Xie, S.; Hor, A. M.; Hu, N. X.; Tripp, C.; Xu, G. *Appl. Phys. Lett.* **1998**, *72*, 756−758.
(7) Aziz, H.; Popovic, Z. D.; Hu, N. X.; Hor, A. M.; Xu, G. *Science* **1999**, *283*, 1900−1902.
(8) Yamada, T.; Zou, D. C.; Jeong, H.; Akaki, Y.; Tsutsui, T. *Synth. Met.* **2000**, *111*, 237−240.
(9) Kervella, Y.; Armand, M.; Stephan, O. *J. Electrochem. Soc.* **2001**, *148*, H155−H160.
(10) Kolosov, D.; English, D. S.; Bulovic, V.; Barbara, P. F.; Forrest, S. R.; Thompson, M. E. *J. Appl. Phys.* **2001**, *90*, 3242−3247.
(11) Schaer, M.; Nuesch, F.; Berner, D.; Leo, W.; Zuppiroli, L. *Adv. Funct. Mater.* **2001**, *11*, 116−121.
(12) Pei, Q. B.; Yu, G.; Zhang, C.; Yang, Y.; Heeger, A. J. *Science* **1995**, *269*, 1086−1088.
(13) Pei, Q. B.; Yang, Y.; Yu, G.; Zhang, C.; Heeger, A. J. *J. Am. Chem. Soc.* **1996**, *118*, 3922−3929.
(14) Manzanares, J. A.; Reiss, H.; Heeger, A. J. *J. Phys. Chem. B* **1998**, *102*, 4327−4336.
(15) deMello, J. C.; Halls, J. J. M.; Graham, S. C.; Tessler, N.; Friend, R. H. *Phys. Rev. Lett.* **2000**, *85*, 421−424.
(16) Mitschke, U.; Bauerle, P. *J. Mater. Chem.* **2000**, *10*, 1471−1507.
(17) Armstrong, N. R.; Wightman, R. M.; Gross, E. M. *Annu. Rev. Phys. Chem.* **2001**, *52*, 391−422.
(18) Riess, I.; Cahen, D. *J. Appl. Phys.* **1997**, *82*, 3147−3151.
(19) deMello, J. C.; Tessler, N.; Graham, S. C.; Friend, R. H. *Phys. Rev. B* **1998**, *57*, 12951−12963.
(20) Maness, K. M.; Masui, H.; Wightman, R. M.; Murray, R. W. *J. Am. Chem. Soc.* **1997**, *119*, 3987−3993.
(21) Lee, J. K.; Yoo, D.; Rubner, M. F. *Chem. Mater.* **1997**, *9*, 1710−1712.
(22) Wu, A. P.; Lee, J.; Rubner, M. F. *Thin Solid Films* **1998**, *329*, 663−667.
(23) Lee, J. K.; Yoo, D. S.; Handy, E. S.; Rubner, M. F. *Appl. Phys. Lett.* **1996**, *69*, 1686−1688.
(24) Lyons, C. H.; Abbas, E. D.; Lee, J. K.; Rubner, M. F. *J. Am. Chem. Soc.* **1998**, *120*, 12100−12107.
(25) Handy, E. S.; Pal, A. J.; Rubner, M. F. *J. Am. Chem. Soc.* **1999**, *121*, 1, 3525−3528.
(26) Wu, A.; Yoo, D.; Lee, J. K.; Rubner, M. F. *J. Am. Chem. Soc.* **1999**, *121*, 4883−4891.
(27) Gao, F. G.; Bard, A. J. *J. Am. Chem. Soc.* **2000**, *122*, 7426−7427.
(28) Rudmann, H.; Kaplan, L.; Sevian, H.; Rubner, M. F. *Abstr. Pap. - Am. Chem. Soc.* **2000**, *220*, 169-PMSE.
(29) Rudmann, H.; Rubner, M. F. *J. Appl. Phys.* **2001**, *90*, 4338−4345.
(30) Buda, M.; Kalyuzhny, G.; Bard, A. J. *J. Am. Chem. Soc.* **2002**, *124*, 6090−6098.
(31) Rudmann, H.; Shimada, S.; Rubner, M. F. *J. Am. Chem. Soc.* **2002**, *124*, 4918−4921.
(32) Liu, C. Y.; Bard, A. J. *J. Am. Chem. Soc.* **2002**, *124*, 4190−4191.
(33) Gao, F. G.; Bard, A. J. *Chem. Mater.* **2002**, *14*, 3465−3470.
(34) Bernhard, S.; Gao, X. C.; Malliaras, G. G.; Abruna, H. D. *Adv. Mater.* **2002**, *14*, 433−436.

10.1021/ja029550i CCC: $25.00

The LECs based on various derivatives of tris(2,2′-bipyridine)ruthenium(II) complexes demonstrate high external quantum efficiency (e.g., up to 2.5% for pristine $Ru(bpy)_3(ClO_4)_2$ films in dc operation using liquid Ga:In or Ga:Sn cathode[27,30,33] and up to 5.5% for $Ru(bpy')_2(bpy'')(PF_6)_2$ (where bpy′ is 4,4′-di-*tert*-butyl-2,2′-bipyridine, bpy″ is 4,4′-di-dinonyl-2,2′-bipyridine) mixed with poly(methyl methacrylate) films in pulsed voltage operation using evaporated Ag cathode).[31] When the devices are prepared under drybox conditions and operated at low luminescence levels (~20 cd/m^2), their stability can be relatively high. However, while operated at a luminescence level as high as 2000 cd/m^2, the light intensity decays to a fraction of its maximum value within minutes. Recent work by Rudmann et al. show that the device lifetime (and to a lesser extent, the quantum efficiency) can be noticeably increased by operating the devices under pulsed voltage (5 V, 50% duty cycle).[29,31] More recently, diffusion of evaporated Al cathode into organic film as a factor of device degradation was reported.[35] However, the mechanism for light-emission decay observed for both liquid (Ga:In or Ga:Sn) and evaporated (Ag or Au) contacts is not clear and remains to be resolved.

In this contribution we discuss the factors causing light-emission decay of the devices based on films $Ru(bpy)_3X_2$ (where X is BF_4^- or ClO_4^-). The stability of the devices prepared and tested in a drybox was compared with those of ones operated in air. Finally, we investigate charge injection and device degradation using fluorescence microscopy on sandwich cell devices and devices with planar gap electrodes. The possible mechanism responsible for $Ru(bpy)_3^{2+}$ device degradation is discussed.

Experimental Section

$Ru(bpy)_3(ClO_4)_2$ was prepared by a metathesis reaction between commercial $Ru(bpy)_3Cl_2$ (Aldrich) and excess sodium perchlorate.[36] $Ru(bpy)_3(BF_4)_2$, $Ru(bpy)_3(PF_6)_2$ and $Ru(bpy)_3(AsF_6)_2$ were prepared using similar procedures with the appropriate sodium or ammonium salts. The resulting crystals were recrystallized from acetonitrile/benzene and dried under vacuum at ~100 °C for several hours. $[Ru(bpy)_2(H_2O)_2](ClO_4)_2$ was prepared according to ref 37 and precipitated with $HClO_4$ instead of $LiClO_4$. It was found, though, that the complex is unstable in air and is oxidized easily to a Ru(III) complex.

Indium−tin oxide (ITO)-covered glass (~20 Ω/□, Delta Technologies) was thoroughly cleaned before device preparation by sonication, first in acetone for 15 min, then for 20 min in a 20−30% (v/v) solution of ethanolamine in highly pure Millipore water at ~60 °C, followed by several rinsing/sonication steps with pure water at room temperature to remove traces of ethanolamine, and dried under a stream of pure nitrogen. Interdigitated electrode arrays (IDAs) using Pt and C as electrode materials were provided by Professor Milena Koudelka-Hep (Institute of Microtechnology, Neuchâtel, Switzerland) and described elsewhere.[38] Small gap Au electrodes were produced by vacuum-evaporating (Denton Vacuum) Au through an "H"-like shadow mask onto glass at 0.1 nm/s while subsequently scratching the gold bridge with either a tapered quartz fiber or a W tip to produce the gap of 2−10 μm.

$Ru(bpy)_3(X)_2$ solutions in acetonitrile were always filtered through 0.2-μm syringe filters before use. Typically, the $Ru(bpy)_3(X)_2$ films (~100 nm) were spin-coated (Headway Research or Specialty Coating Systems) from a 4% (m/v) acetonitrile (Aldrich) solution at 1000−2000 rpm, onto clean ITO-covered glass or other substrate. After spin-coating, the device was dried under vacuum for at least 8 h at 100−120 °C. Ga:Sn or Ga:In (Alfa-Aesar) liquid contacts were printed using a syringe. The current−light emission−voltage curves were taken using an AUTOLAB electrochemical station coupled with a Newport optical power meter. Measurements were performed at room temperature (25 °C) under ambient conditions, or in a drybox (MBraun) under a nitrogen atmosphere. All operations in the drybox were performed with water and oxygen concentration not exceeding 1 ppm each. For the measurements performed in the drybox, the films were spin-coated, dried, and tested under nitrogen, in the same drybox, without being exposed to air. Note that unlike some earlier reports from this laboratory,[27,33] in the measurements in air, the cathode contact was not sealed with epoxy cement. The preparation conditions for each particular device are specified in the text.

All current and light emission vs voltage or current and light emission vs time measurements reported here are only from devices that were free from ohmic shorts that can result from penetration of the contact material through defects in the film. The quantum efficiency was always measured during the first scan, taken immediately after contacts were made. In all reported electrical measurements, positive bias was applied to the ITO electrode.

Optical microscopy was carried out in air using a Nikon TE 300 inverted microscope using a MicroMax 1024B (Roper Scientific) or a Nikon DXM thermoelectrically cooled digital CCD camera. All photoluminescence (PL) images were taken using 460−490 nm (excitation) and 520 nm (emission) filters.

Results and Discussion

The $Ru(bpy)_3^{2+}$ LECs and the mechanism of electroluminescence (EL) is based on recombination of $Ru(bpy)_3^{3+}$ and $Ru(bpy)_2(bpy^-)^+$ species (which in further discussion will be referred as "holes" and "electrons", respectively) leading to the appearance of the $Ru(bpy)_3^{2+*}$ excited state, followed by light emission with a maximum around 660 nm.[24,30] Essentially, it is the same mechanism that was proposed for electrogenerated chemiluminescence (ECL) of $Ru(bpy)_3^{2+}$ in solution.[39,40]

Typical voltage scans for the $Ru(bpy)_3(BF_4)_2$ devices taken in a drybox and in air are shown in Figure 1. Plotting the current on a logarithmic scale allows observation of two current regions which can be described in terms of the consecutive injection of holes and electrons into the device.[30] For the device measured in a drybox the unipolar injection of the first charge carrier begins at 1 V (precision in measurement of the initial current levels is restricted by the sensitivity of the potentiostat), i.e., considerably below the potential corresponding to the optical gap of $Ru(bpy)_3^{2+}$, where the optical gap is taken as the electroluminescence maximum typical for ITO/~100 nm $Ru(bpy)_3(ClO_4)_2$/Ga:In devices (660 nm or 1.88 eV). In the region between 1.5 and 2 V the current flattens and no longer follows an exponential relationship. At voltages a little above 2 V, the change in the slope of log(I) versus V indicates injection of the second carrier concurrent with light emission. Comparable $I-V$ curves are also observed for devices tested in air, although the potential needed for the first carrier injection for such an LEC is larger, and the separation between the two waves disappears (note a change in slope around 2 V in Figure 1, dashed $I-V$ curve). This effect may be due to oxidation of the liquid metal contact resulting in an oxide layer between metal and organic

(35) Rudmann, H.; Shimada, S.; Rubner, M. F.; Oblas, D. W.; Whitten, J. E. *J. Appl. Phys.* **2002**, *92*, 1576−1581.
(36) McCord, P.; Bard, A. J. *J. Electroanal. Chem.* **1991**, *318*, 91−99.
(37) Hogan, C. F.; Forster, R. J. *Anal. Chim. Acta* **1999**, *396*, 13−21.
(38) Fiaccabrino, G. C.; Koudelka-Hep, M. *Electroanalysis* **1998**, *10*, 217−222.
(39) Tokel, N. E.; Bard, A. J. *J. Am. Chem. Soc.* **1972**, *94*, 2862−2863.
(40) Tokel-Takvoryan, N. E.; Hemingway, R. E.; Bard, A. J. *J. Am. Chem. Soc.* **1973**, *95*, 2862−2863.

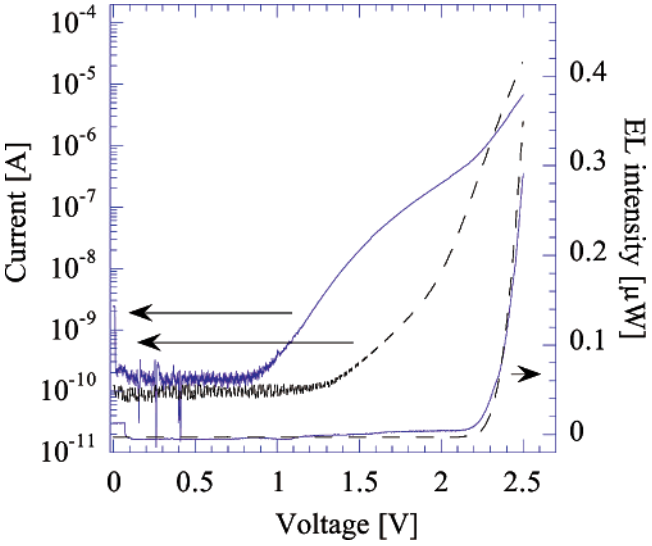

Figure 1. Typical current−voltage and EL intensity−voltage characteristics for ITO/$Ru(bpy)_3(BF_4)_2$/Ga:Sn devices tested in a drybox (solid lines) and in air (dashed line). Voltage scan speed was 20 mV/s. For both the measurements the same $Ru(bpy)_3(BF_4)_2$ film (~200 nm thickness) was used.

film, thus impeding charge injection at lower potentials. While the shape of the $I-V$ curves for the devices measured in a drybox always contained two waves, the shape for the ones tested in air could be different for different devices.

The sequence of electron or hole injection as well as their relative mobilities will be discussed in detail below. Qualitatively, similar behavior is also observed for other $Ru(bpy)_3(X)_2$ LECs, e.g., where X = ClO_4^-, PF_6^-. However, with these anions, a slower scan speed needed to be applied to properly resolve the waves since the response time of the devices made with larger counterions is considerably longer.[30,31]

Effect of Unipolar Injection on LEC Stability. Our basic assumption was that the effects of hole or electron injection on device stability may be different. Figure 2 shows the effect of passing the same charge (6.8 mC) at voltages corresponding to unipolar (1.65 V) and bipolar (2.5 V) injection through the same $Ru(bpy)_3(BF_4)_2$ device on device behavior. The EL intensity−voltage responses of the device in its initial state, and after passing 6.8 mC in unipolar regime (Figure 2 b) are nearly identical, indicating that the device did not undergo any significant degradation during the unipolar injection. The slightly larger current in the region of unipolar injection after passing the charge (compare dashed and dotted lines in Figure 2 a) is probably due to formation of a persistent concentration gradient of BF_4^- across the device (it took 20 000 s to pass 6.8 mC at 1.65 V). At voltages 2.5 V and greater the current practically coincides with that of the pristine LEC.

Passing the same charge at 2.5 V only took 115 s and led to a noticeable decrease in the EL intensity (by about a factor of 2 at 2.5 V), while the current in the region of bipolar injection remained almost the same. Interestingly, the unipolar injection with the device that had been subjected to 2.5 V started at ca. 200 mV higher voltage (compare solid and dotted lines in Figure 2 a). This observation may indicate formation of a partially insulating zone, either in the bulk of the film or near one of the interfaces (see below).

Thus, this experiment suggests that unipolar injection is not responsible for device degradation (at least under drybox

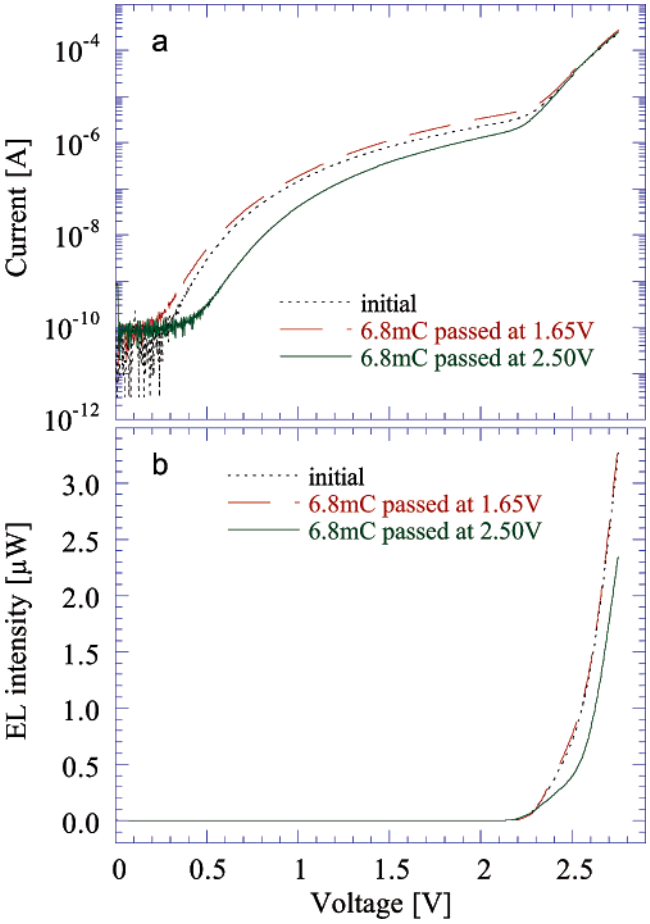

Figure 2. Current (a) and EL intensity (b) vs voltage for ITO/$Ru(bpy)_3(BF_4)_2$/Ga:Sn device in its initial state (dotted line), after passing 6.8 mC at 1.65 V (dashed line) and after passing 6.8 mC at 2.5 V (solid line). Voltage scanning speed was 20 mV/s. The device was prepared and tested in a drybox. Before each measurement the LEC was held at 0 V for 45 s.

conditions). It necessarily implies that *the prerequisites of device degradation involve either the injection of the second charge carrier or the production of the* $Ru(bpy)_3^{2+*}$ *excited state.*

Comparison of Device Stability in Air and Drybox (Electrical Characteristics Study). In a previous study,[30] we reported that response times (which was defined as the time to reach maximum EL intensity at a certain voltage) of the $Ru(bpy)_3(X)_2$ LECs, where X= BF_4^-, ClO_4^-, PF_6^-, AsF_6^-, were considerably shorter when a device is tested in air compared to the results obtained in a drybox. The difference in response times was proposed to be related to atmospheric moisture, which increases counterion mobility (a generally observed phenomenon for solid electrolytes).[30] The difference in response times between the devices tested in air and in the drybox decreases in the row BF_4^- > ClO_4^- > PF_6^- > AsF_6^- probably because ion transport in solids is affected by the solvation shell to a larger extent for small ions than for big ones.

To compare the LECs tested in air and the drybox, we checked dozens of devices fabricated on the same film of $Ru(bpy)_3(BF_4)_2$ (i.e. different cathode contacts on the same film over a single piece of ITO), which was prepared and dried in the drybox. The first group of devices was tested in the drybox, then the film was exposed to the ambient environment and the second group of LECs was prepared and tested. An example of current and light emission transients for a single $Ru(bpy)_3(BF_4)_2$

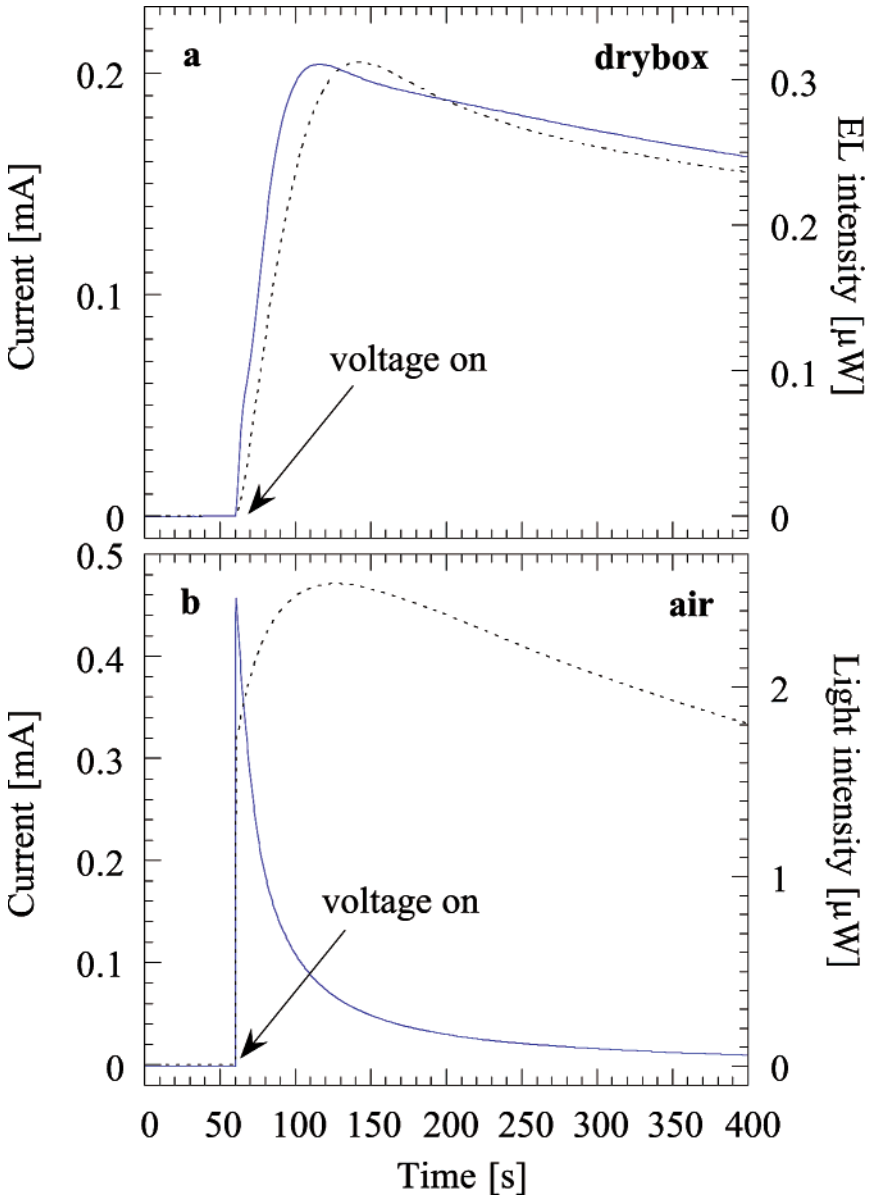

Figure 3. EL intensity (solid line) and current (dotted line) vs time for ITO/Ru(bpy)$_3$(BF$_4$)$_2$/Ga:Sn device tested at 2.75 V: (a) in drybox; (b) in air. The same ITO/Ru(bpy)$_3$(BF$_4$)$_2$ film was used in (a) and (b), with different Ga:Sn contacts at two different locations on the film.

device first measured in the drybox and then in air (with a new Ga:Sn drop) is shown in Figure 3 a, b, respectively. For the device measured in the drybox, the maximum of EL intensity is reached in ca. 52−60 s, while the device measured in air takes ca. 0.4−0.8 s. Since the response times are so different, a simple comparison between lifetimes of the same device tested in air and in the drybox at the same voltage is not adequate.

Therefore, as a criterion for comparison of the devices tested under different conditions, we used the number of photons (integrated EL intensity) emitted from the moment the voltage was applied, to the time where the EL intensity dropped to one-fifth of its maximum value. Before each transient measurement, current−voltage and EL intensity−voltage curves were taken and later used as a reference to find the relative device area determined by the cathode contact (surface area of the devices could not be directly measured in the drybox).

Maximum quantum efficiency (QE) values extracted from these curves are shown in Figure 4 a. The average of QE values for the LECs tested in air are about 2 times higher than that for devices tested in the drybox. This result suggests that the presence of either water or oxygen somehow makes charge carrier injection into the film more balanced. Figure 4 b shows that the dependence between integrated EL intensity and charge passed through the LECs is close to linear (on log−log coordinates) despite the fact that the LECs were tested at various voltages. Apparent separation between the points corresponding to the devices tested in air and the drybox demonstrates the clear effect of an inert environment of the device's longevity, while the fact that both sets of data lie practically on the same line indicates that the charge transfer and, hence, the EL generation in air and the drybox probably follow the same reaction mechanism.

Plots c and d in Figure 4 respectively show integrated EL intensity and device lifetime as a function of applied voltage in the drybox and in air. In both environments the integrated EL intensity increases in the range 2.25−2.75 V, and then reaches a plateau (possibly after a not well-defined maximum). The average integrated EL intensity (as well as the device lifetime)

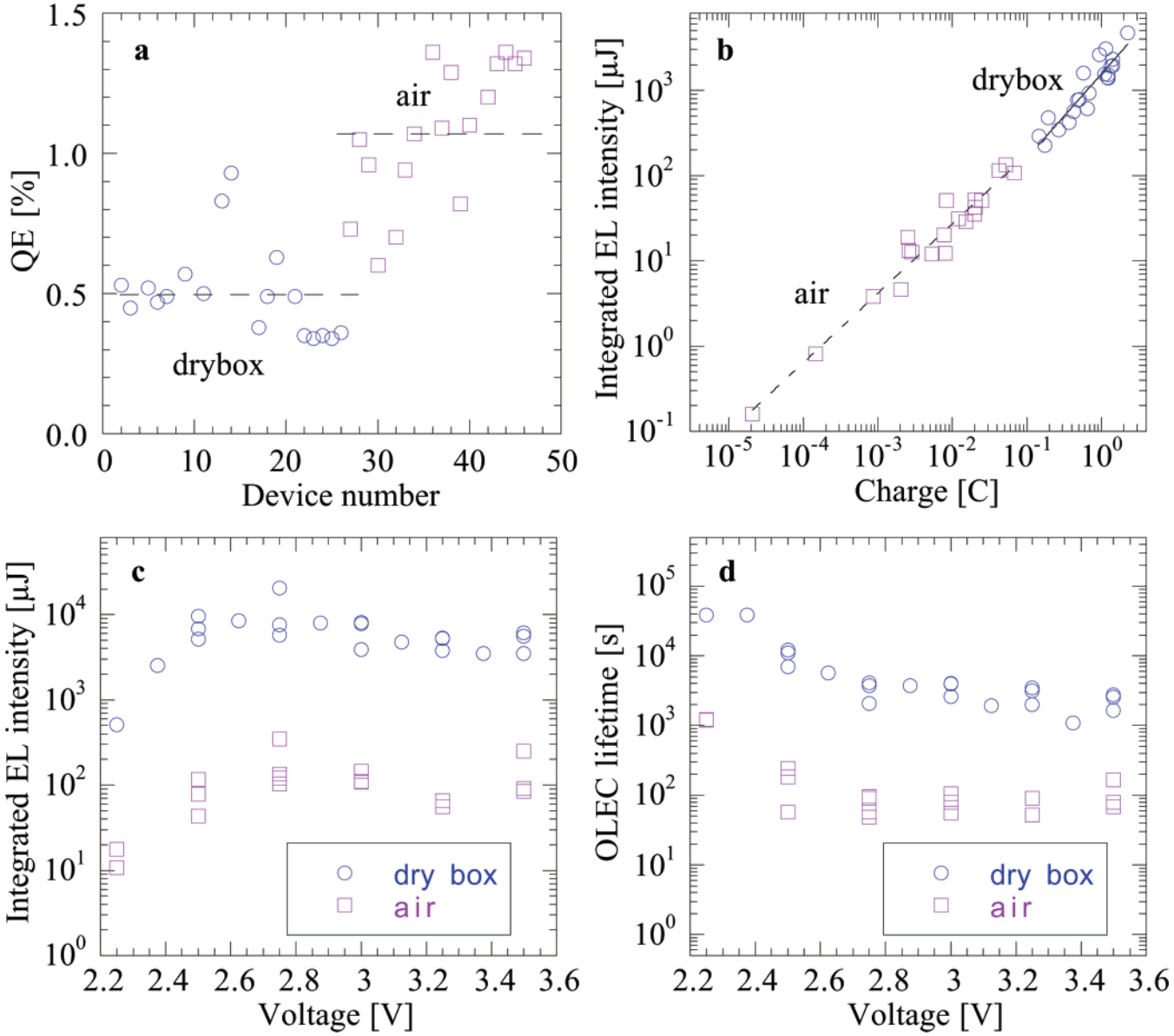

Figure 4. (a) Maximum quantum efficiency (QE) for LECs tested in drybox and air; dashed line shows the mean QE for both sets of data; the QE values were extracted from current−voltage and EL intensity−voltage curves (not shown). (b) Integrated EL intensity vs charge passed; each point corresponds to a device tested at a voltage ranging between 2.25 and 3.5 V. (c, d) Integrated EL intensity and device lifetime vs voltage for LECs tested in drybox (O) and in air (□); the EL intensity data were corrected for discrepancy in the device surface area using a factor extracted from the LEC current−voltage response. Integrated EL intensity, charge and device lifetime in (b−d) were defined at the point where EL intensity reached one-fifth of its maximum value. For all the measurements the same $Ru(bpy)_3(BF_4)_2$ film (~200 nm thickness) was used.

for the LECs tested in the drybox is approximately 2 orders of magnitude higher than that for those tested in air, pointing again to the negative effect of water or oxygen on device stability. The fact that there is no prominent decline of integrated EL intensity with voltage suggests the absence of side electrochemical reactions that occur at higher potentials and lead to the device degradation. For example, a possible reaction is the additional reduction of $Ru(bpy)_2(bpy^-)^+$ into $Ru(bpy)(bpy^-)_2^0$ followed by decomposition of the latter. However, if this had happened, at higher voltages the degradation processes would have been accelerated, leading to the decrease in the total amount of emitted photons. Since this is not observed (Figure 4 c), side electrochemical reactions (such as the successive reduction of $Ru(bpy)_2(bpy^-)^+$ or the successive oxidation of $Ru(bpy)_3^{3+}$) at higher potentials may be excluded from consideration. A similar argument is applicable to some destructive second-order reactions, e.g., to irreversible annihilation of the excited state ($Ru(bpy)_3^{2+*} + Ru(bpy)_3^{2+*} \rightarrow Ru(bpy)_3^{2+} + X$ where X is some nonluminescent byproduct). The rate of such a reaction would be low at low potentials and would be increased with a rise of voltage following the current growth, resulting in a decrease of integrated EL intensity with voltage. This does not happen; thus, *we can hypothesize that the LEC degradation (Figure 3) is caused by some first-order, irreversible reaction of either* $Ru(bpy)_3^{3+}$, $Ru(bpy)_3^{+}$, *or* $Ru(bpy)_3^{2+*}$ *species assisted by either atmospheric moisture or oxygen.* The chemistry of degradation is discussed in more detail in a later section.

Microscopic Study of the LECs during Their Operation. Operation of $Ru(bpy)_3^{2+}$ LECs either in air or in the drybox leads to a decrease in fluorescence, indicating that device degradation is due to some irreversible chemical processes occurring in the $Ru(bpy)_3^{2+}$ films. However, typically for the

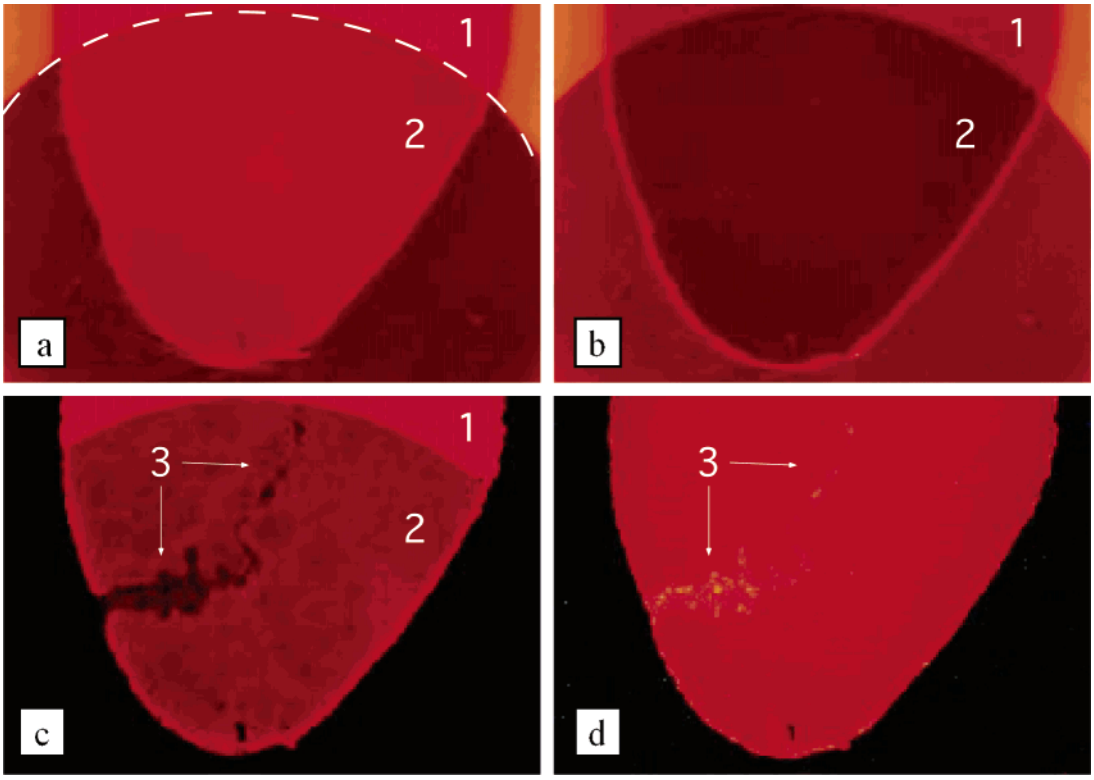

Figure 5. Microscopic images of ITO/$Ru(bpy)_3(ClO_4)_2$/Ga:Sn device prepared and sealed with epoxy in the drybox. (a, b) PL images of the device before and after operation (2 h at 3 V), respectively (exposure time in both cases is 0.067 s). (c) EL image of the device taken ~5 s after applying 3 V bias (exposure time is 0.067 s). (d) EL image of the device taken ~2 h of operation (exposure time is 25 s). The dark region 2 seen in (a−c) was created by illumination with 460−490 nm light of the epi-fluorescence module of the microscope (Hg lamp) for ~2 min. The contour of region 2 is pointed out in (a) with a white dashed line. The contour of Ga:Sn contact is clearly seen in (c, d).

devices tested both in drybox and air, while the EL intensity decreases by at least 2 orders of magnitude from its maximum value, the fluorescence intensity drops only by a factor of 1.5−3. Panels a and b of Figure 5 show the photoluminescence (PL) images of the same ITO/$Ru(bpy)_3(ClO_4)_2$/Ga:Sn device (prepared and sealed in the drybox) before and after operation. Before applying voltage to the device, part of it was intentionally irradiated (as described below in the PL decay study) with a spot of intense blue light (region 2 in Figure 5 a, b). The PL intensity of the device after operation for 2 h was ca. 2 times smaller than the one of pristine device both in regions 1 (not photolyzed) and 2. However, this relatively small change in PL corresponds to a change in the EL intensity of at least 2 orders of magnitude initially and after 2 h of operation, as can be seen from comparison of exposure times used for acquisition of the images shown in Figure 5, c and d. We suggest that the reason for the observed phenomenon is that *device degradation occurs in a relatively thin layer of the* $Ru(bpy)_3^{2+}$ *film which probably corresponds either to the recombination zone or to the zone where one of the carriers is injected*. Experiments with planar LECs (see below) confirm this hypothesis.

Interestingly, the difference between pristine and photolyzed areas of the device (regions 1 and 2 respectively), which is clearly seen in the fluorescence images of the device (Figure 5 a, b) as well as in the electroluminescence image taken ~5 s after applying bias (Figure 5 c), gradually fades away in following electroluminescence images (not shown) and disappears completely in the images taken after a few hours of operation (Figure 5 d). To explain this phenomenon, one more experimental fact should be mentioned. Illumination of the functioning $Ru(bpy)_3^{2+}$ LEC with intense blue light (the same light source was used for photoexcitation of region 2 shown in Figure 5 a, b) leads to a 20−50% decrease of the current passing through the device (because of an increase of the film resistance). When a bias is applied to the LEC, current preferentially passes through the more conductive unphotolyzed part of the device (region 1 in Figure 5 c), resulting in both brighter electroluminescence and faster device degradation (compared to photolyzed region) in this region. Thus, during operation, the EL intensity drops faster in the pristine region of the device until ultimately the difference between regions 1 and 2 (Figure 5 d) disappears. However, in some analogous experiments the difference did not completely fade away. In some cases, EL in the photolyzed region at a certain moment of device operation became brighter than in the pristine part of the device, depending on the potential at which the device was operated, the duration of photoexcitation, and the time at which the image was taken.

Infrequently, different EL intensities were observed in images of the functioning $Ru(bpy)_3^{2+}$ LEC with no connection to preliminary photolysis. For example, region 3, unnoticeable in the PL image of the device before operation (Figure 5 a), is clearly seen as an irregular dark feature in the EL image in Figure 5 c. The opposite behavior is observed in Figure 5 d where region 3 shows the brightest feature at the end of the device lifetime. The most probable reason for this (as in the case of photolysis) is that there are certain parts of the film with a conductivity that is different from the bulk of the device. In such a region, the time to reach the EL intensity maximum is longer, and emission decay takes a longer time as well; thus,

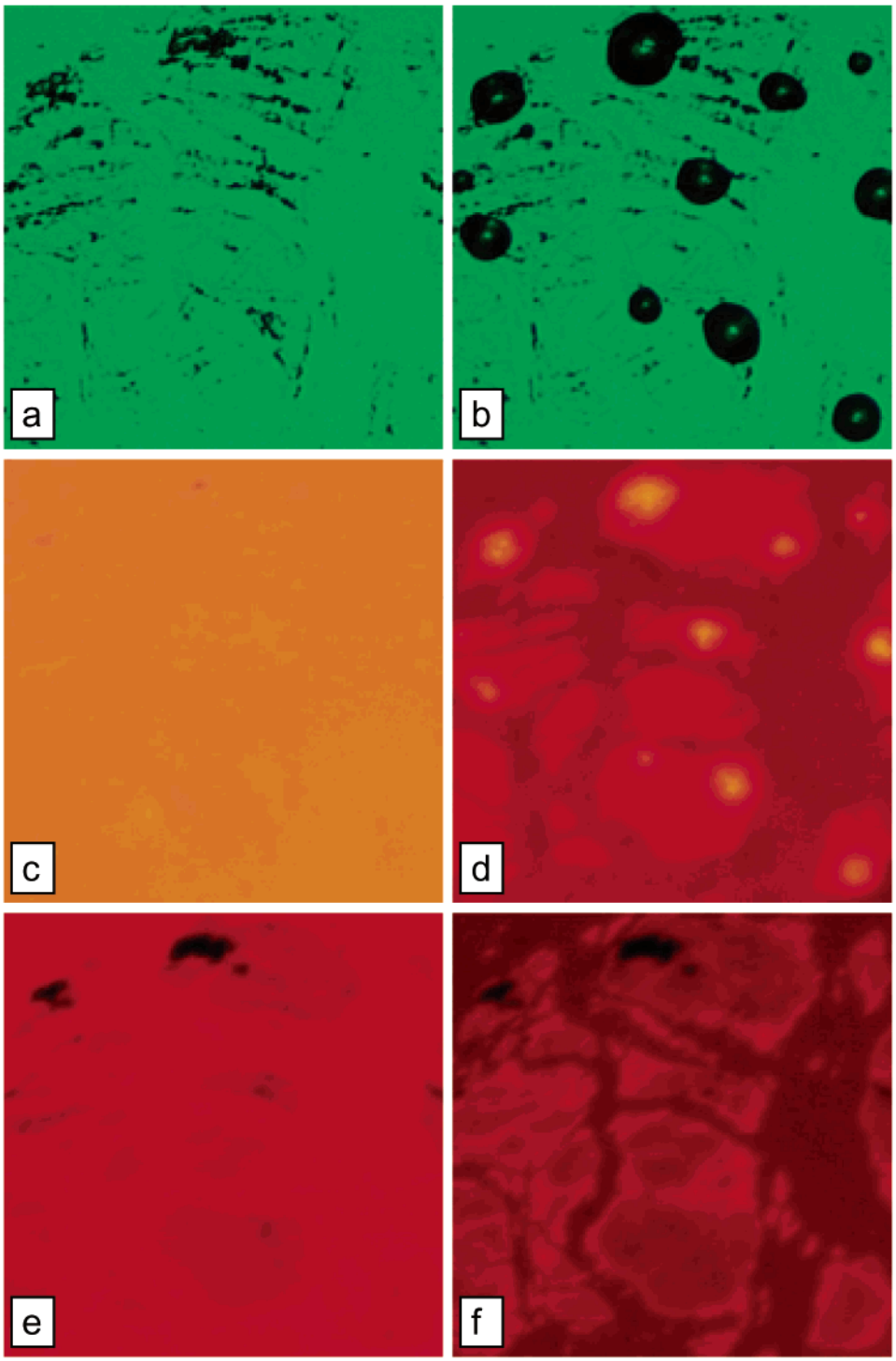

Figure 6. Microscopic images of a part of ITO/$Ru(bpy)_3(ClO_4)_2$/Ga:In device prepared and tested in air. (a, b) Reflectance images of the device before and after operation respectively. (c, d) PL images of the device before and after operation respectively (exposure time is 0.067 s). (e) EL image of the device taken ~5 s after applying 2.25 V bias (exposure time is 0.067 s). (f) EL image of the device taken after ~30 s of its operation (exposure time is 0.167 s). Orange-yellow color observed in (c) and partially in (d) is due to overexposure. Images (b) and (d) were taken after ~40 min of device operation at 2.25 V bias.

at a certain time, the EL intensity in this region (Figure 5 d) becomes greater than in the surrounding areas of the film, which had already become darker. A higher resistivity in different parts of the $Ru(bpy)_3^{2+}$ film may imply either a decrease of mobility for one or both carriers, yielding a decreased EL intensity in these regions.

Figure 6 a−d shows reflectance and PL images of an ITO/$Ru(bpy)_3(ClO_4)_2$/Ga:In device before and after operation in air. As with the sealed device, the PL intensity after extended operation dropped by a factor of 1.5−3, while the drop in EL intensity is at least 360 times (estimated from the difference in image brightness and exposure time; the EL image at the end

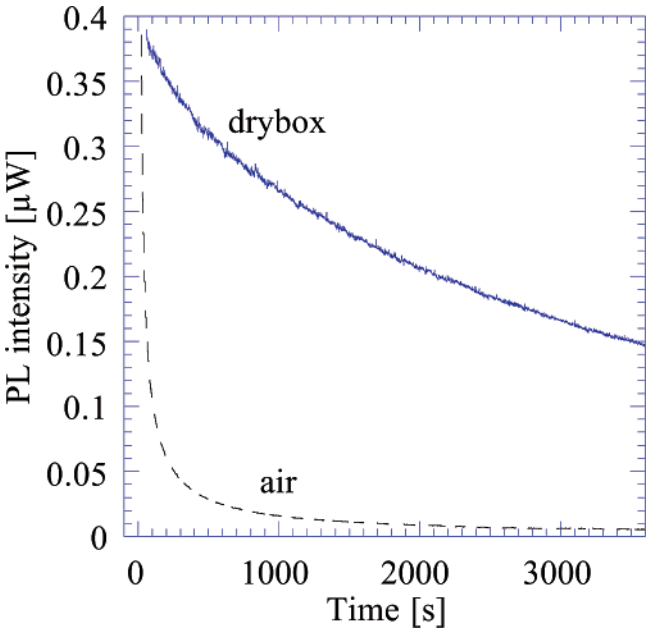

Figure 7. PL decay of $Ru(bpy)_3(ClO_4)_2$ film observed in nitrogen (solid line, prior to measurement the film was sealed in the drybox) and air (dashed line). The intensity of the excitation source (460−490 nm part of the spectrum of Hg lamp) was ~3 mW. Very similar results are observed for other $Ru(bpy)_3(X)_2$ films.

of device operation is not shown). During operation in air, $Ru(bpy)_3^{2+}$ LECs often (although not always) form "bubbles" (compare Figure 6 a and b). The bubble formation occurs in the areas where air was trapped during contacting the film with liquid alloy. However, only a small fraction of existing areas with trapped air generates the bubbles. The EL intensity in the areas adjacent to trapped air is lower in the beginning of the device operation (Figure 6 e), implying a higher resistivity. After some time, when the light in the device in the areas free of trapped air had decayed, the relative intensities became reversed (Figure 6 f), i.e., EL intensity was higher in the areas containing trapped air and where bubbles formed. A PL intensity image (Figure 6 d) shows that in these areas the film remains relatively intact (especially under the bubbles where the least amount of charge has been passed). The nature of the bubbles is currently unclear; a possible explanation could be that bubbles consist of hydrogen evolved in electrolysis of water present in air on the liquid metal cathode. Nevertheless, the bubbles cannot be the main factor causing $Ru(bpy)_3^{2+}$ LEC degradation in air since *the maximum EL emission as well as the maximum drop in PL intensity occurs in the areas free of the defects*. Devices with the cathodic contact covered with epoxy cement did not show this bubble formation.

PL Decay of $Ru(bpy)_3^{2+}$ Films. During microscopic studies of the operation of $Ru(bpy)_3^{2+}$ LECs it was noticed that under illumination with the Hg lamp of the microscope (with band-pass filter of 460−490 nm matching the absorption maximum of $Ru(bpy)_3^{2+}$) the PL of the films decayed rapidly. As with the EL decay for these films, the decay kinetics was strongly affected by environmental conditions as shown in Figure 7. The resemblance between both absolute values of PL and EL and the character of their decay (compare Figure 7 with Figure 3) suggests that *both photo- and electroluminescence decay may have the same origin related to some irreversible side reaction of $Ru(bpy)_3^{2+*}$ species assisted by either atmospheric moisture or oxygen*. After formation of the excited state, its decay path is clearly not dependent on how the $Ru(bpy)_3^{2+*}$ was generated. This hypothesis is in good agreement with the microscopic study of the functioning OLEDs discussed above, where the largest PL decay was observed in those areas where most of the photons were emitted. A study distinguishing the role both oxygen and water play in the PL and EL decay processes is currently in progress.

Microscopic Study of the LECs in Planar Configuration. An alternative to the conventional sandwich configuration is a planar (interdigitated array) configuration of the electrodes for LECs, as long as the spacing is sufficiently small that currents flow at reasonable voltages. In this arrangement one can study EL profiles between the electrodes of the device during operation and as it undergoes degradation processes. This approach was used by Pei and co-workers, who studied the EL profile of thin layers of poly(1,4-phenylenevinylene) (PPV) mixed with poly(ethylene oxide) (PEO)/$LiCF_3SO_3$ spin-coated onto a glass substrate prepared with parallel Au electrodes (spaced 15 μm apart).[12,13] The same approach can be used for $Ru(bpy)_3^{2+}$ films, although closer spacings are needed because they are less conductive than PPV films. A motivation for this study is in determining the order in which carriers are injected into $Ru(bpy)_3^{2+}$ films. As stated above (see discussion of Figure 2), the carrier that is injected at potentials below 1.8 V alone is not responsible for the device degradation; thus, understanding the nature of the carriers is important for elucidating the degradation mechanism. Rudmann et al. hypothesized that injection of electrons occurs first due to the presence mixed-valent $Ru(bpy)_3^{2+}/Ru(bpy)_2(bpy^-)^+$ states caused by interaction with their evaporated Al cathode.[35] In our previous work, electrons were also suggested as the first carrier injected since this assumption was necessary to match experimental current−voltage data with the proposed model.[30] However, the calculation was carried out under the assumption that the mobilities of both carriers are equal, which may not be true. Unipolar injection was also observed in devices with liquid metal contacts, as discussed above; therefore, metal apparently does not diffuse into the film. For devices based on Au, Pt, and C electrode interdigitated arrays (IDAs), as discussed below, diffusion of electrode material into the film is also very unlikely.

The traditional method of determining the type of carrier and its mobility would be to build a field effect transistor (FET) with $Ru(bpy)_3^{2+}$ films and to study the current dependence on gate voltage. This approach is currently underway. An alternative way of studying the charge injection into $Ru(bpy)_3^{2+}$ films is to analyze the EL and PL profile of the film placed between electrodes in the planar configuration. Figure 8 a shows a reflectance image of a carbon electrode IDA covered with a film of $Ru(bpy)_3(ClO_4)_2$. In all IDA images described here, the electrodes, 2 μm wide, are the dark lines, with the positive electrodes extending from the left side of the image and the negative electrodes (one of them is indicated by a black arrow) from the right. The Si_3N_4 interelectrode spacing was 2 μm.

When a voltage (7.5 V) is applied to the IDA, an EL profile is observed (Figure 8 b−d and Figure SI 1). From the first frame where EL can be detected (Figure 8 b) light is clearly seen to be emitted from the areas adjacent to negatively charged electrodes. After reaching its maximum (Figure 8 c), the EL gradually decayed (Figure 8 d) and finally disappeared, with

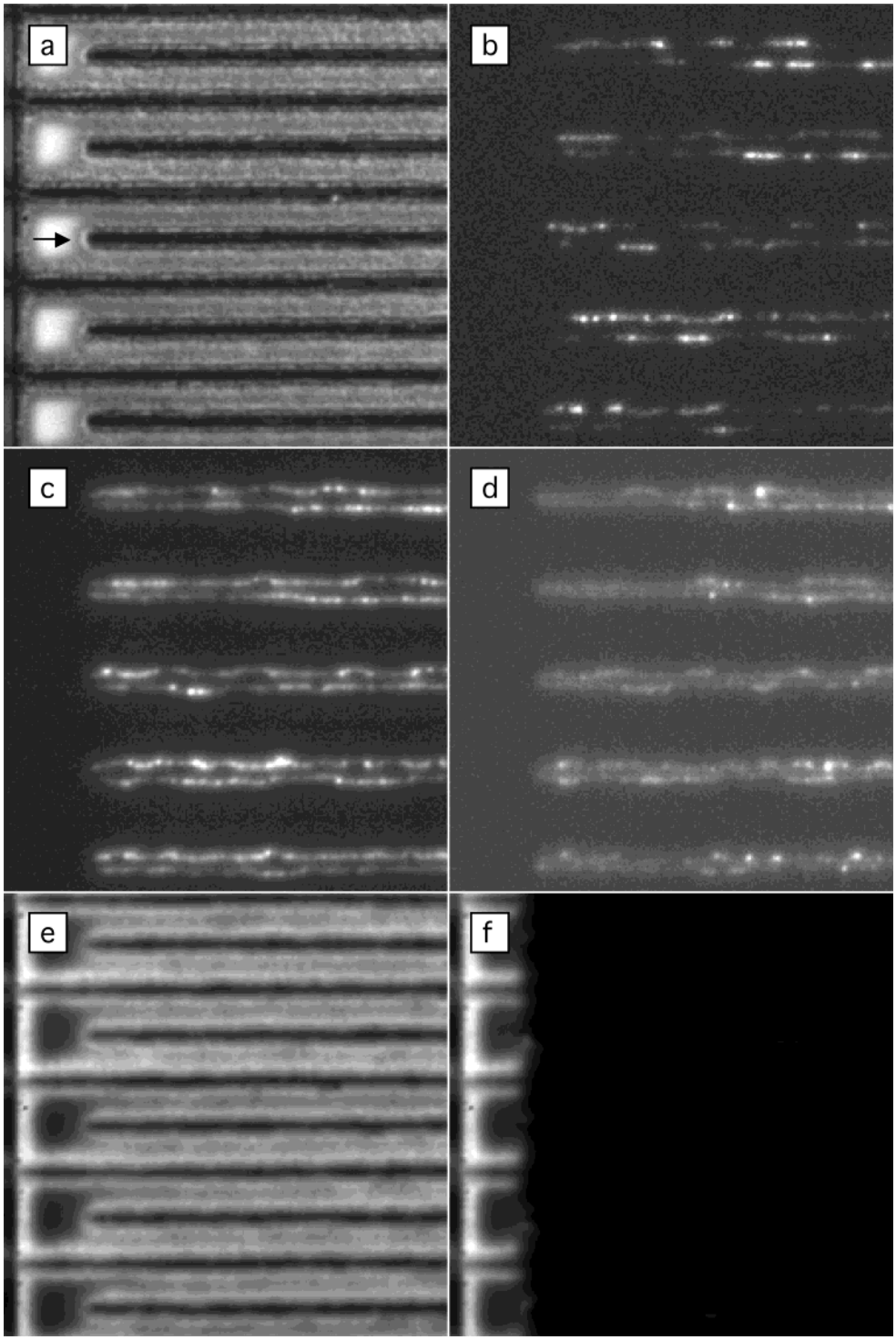

Figure 8. Microscopy of a region of carbon IDA with $Ru(bpy)_3(ClO_4)_2$ film. (a) Reflectance image where bright features correspond to Si_3N_4 spacing separating darker carbon lines. (b) EL image of the same region after 7.5 V was applied to the IDA (second frame). (c) Successive EL image (3d frame). (d) Successive EL image (fifth frame). (e) PL image before operation. (f) PL image taken immediately after operation. Exposure time in (b−d) was 15 s and intensity scale was arbitrarily chosen for each image. See Figure SI 1 for all 23 frames with specified intensity scale. The width of carbon finger electrodes is 2 μm. In this experiment, negative bias was applied to electrodes pointed out by black arrow (a).

the exception of a few spots (see Figure SI 1 for the entire time series). Interestingly, within the EL profile, the light intensity varied significantly, with some bright spots (i.e., in Figure 8 b) where the EL intensity was 10 times higher than the average level. The possible reasons for this are discussed below. Comparison of Figures 8 b−d also reveals that EL profile moved with time even more toward the cathode; in Figure 8 d most of the EL was observed right above the cathode, suggesting that charge injection during device operation at constant voltage became more unbalanced. This effect clearly contributed to the change of the LEC efficiency with time, as well as to the rate of EL decay, and provides a logical explanation of considerably longer lifetimes observed by operating the devices under pulsed voltage.[29,31]

The fact that the EL is observed in the areas adjacent to cathodes suggests either that holes have a considerably higher

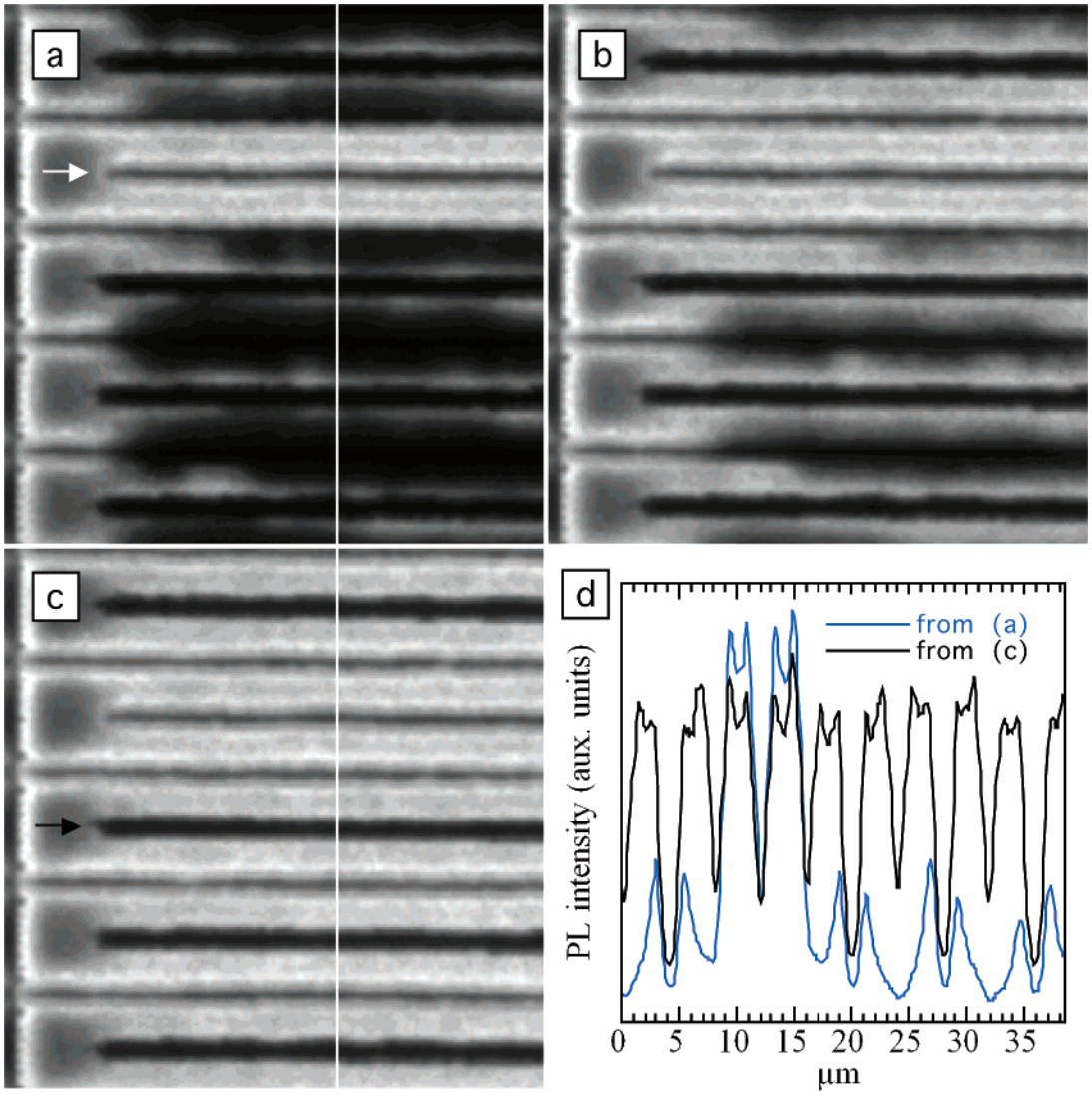

Figure 9. (a−c) Successive PL images (1st, 10th, and 21st frames respectively) taken from a region of carbon IDA with $Ru(bpy)_3(ClO_4)_2$ film after Figure 8f, where the device was held at 3.5 V for 10 min; after short-circuiting the cell. (d) PL profile taken from (a) and (c) at the location specified by white line. Images (a−c) were acquired with exposure time 5 and 20 s delay between frames; intensity scale was arbitrarily chosen for each image. See Figure SI 2 for all 21 frames with specified intensity scale. The width of carbon finger electrodes is 2 μm. In this experiment negative bias had been applied to electrodes pointed out by black arrow (c). The contact to the electrode pointed out with a white arrow was missing due to a defect in the IDA (not shown) so it can be used for comparison with other electrodes; the difference in PL intensity at the defective line between (a) and (c) shown in (d) is due to the film photolysis during image acquisition.

mobility than do the electrons or that the charge injection is not balanced (favoring hole injection) or both. Our preliminary results on FETs based on $Ru(bpy)_3^{2+}$ films indicate that holes are the major carriers for operating voltages of more than 3 V.[41] Although this confirms the hypothesis of highly unbalanced charge injection into $Ru(bpy)_3^{2+}$ LECs, the relative mobilities of holes and electrons in these devices still have to be elucidated.

The following procedure was used to determine which charge carrier is injected at the low bias corresponding to unipolar injection with C and Au IDA $Ru(bpy)_3^{2+}$ LECs (not shown): In these experiments, prior to applying a voltage necessary to generate EL (3−9 V), the voltage below 2 V was applied for a few minutes, and the unipolar injection current (e.g., see Figure 1) was observed. Then, a higher voltage was applied and EL was detected. If electrons had been injected first, passing through the device in the unipolar region (applied voltage lower than 2 V), then after a higher voltage was applied, the first EL detected would have been observed at or near the anode. However, in each of these experiments there was no noticeable difference in the location of EL (compared to the images shown in Figure 8 b−d where the voltage of 3−9 V was applied from the beginning), which was always observed near the cathode. This implies that the holes are injected first. However, there is still a possibility that the number of unipolar electrons injected (with the assumption that electrons are the first injected carrier) is so small (the currents observed in the unipolar region are 0.1−1 nA) that, when the higher voltage is applied (to induce bipolar injection), the resulting EL near the anode is below the CCD detection limit.

Panels e and f in Figure 8 compare the PL intensity of $Ru(bpy)_3(ClO_4)_2$ film in a device before and after an EL experiment. The PL image of the film before operation was not uniform and was generally similar to the reflectance image because of film thickness variations following the morphology

(41) Kalyuzhny, G.; Pile, D.; Khondaker, S.; Bard, A. J. Unpublished experiments.

of the IDA surface and difference in reflectivity of the carbon electrodes and the Si_3N_4 interelectrode spacing (compare a and e of Figure 8). Device operation caused a considerable (ca. 4−5 times) drop in PL intensity in the regions where current is apparently flowing (Figure 8 f). As follows from the EL profile, most of this current resulted from hole injection. Therefore, the possible reasons for the PL decay are either a decrease in the concentration of the luminescent $Ru(bpy)_3^{2+}$ (since generated $Ru(bpy)_3^{3+}$ is not luminescent) or quenching of $Ru(bpy)_3^{2+*}$ by $Ru(bpy)_3^{3+}$ or another generated quencher (or a combination of both of these factors).

This change in PL was not permanent. Figure 9 and Figure SI 2 show a sequence of the PL images taken after device operation when the contacts were short-circuited.[42] The device exhibited full recovery of PL in the areas near the electrodes that were positively charged during device operation. The image shown in Figure 9 a was taken at about 3 min after the end of device operation and 1 min after the device was short-circuited, so that a considerable part of PL intensity had been already recovered (compare Figures 9 a and 8 f). We intentionally show the section of the IDA where connection to one of the electrode fingers (the electrode indicated by a white arrow) was missing due to a defect located at a different region of the IDA (not shown), and thus the contrast between it and rest of the electrodes is clearly seen. Figure 9 c, d shows that the PL intensity at the cathodes is noticeably lower than that at the corresponding anodes where PL intensity is barely discernible from the unconnected electrode. This change did not disappear for weeks and appears to indicate permanent device degradation. The presence of the region with lower PL intensity at the cathode confirms the previous hypothesis that in sandwich LECs the degradation occurs in a relatively thin layer.

Impedance data show that resistance between the electrodes on the IDA with the $Ru(bpy)_3^{2+}$ film increased as a result of device operation after the device reached steady state (Figure 10). It generally takes days to reach the resistance steady state after device operation if the device is left open-circuited. Short-circuiting the device cuts down the time necessary for reaching the steady state to 5−15 h.

The resistance of the device measured immediately after turning off the voltage was noticeably lower than that of the pristine film, indicating that the partially charged $Ru(bpy)_3^{3+}$/$Ru(bpy)_3^{2+}$ film existing during device operation exhibits a higher conductivity, probably due to an increase of charge carrier concentration. This effect can amplify unevenness in the current flow through the film since, once the passing current decreases resistance in a certain path, the current will continue to rise due to a positive feedback. This may serve as an explanation of the presence of the "hot spots" in EL profile of planar LECs (Figure 8 b−d). The decrease in resistivity of the film facilitating hole transfer may also explain the shift of EL profile toward the cathode during device operation as observed in Figure 8 b−d. Since PL microscopy data from both sandwich and planar LECs indicate that the changes in the device PL intensity are observed only in a thin layer near the cathode, the increase of the device resistance resulting from its operation probably occurs in the same place.

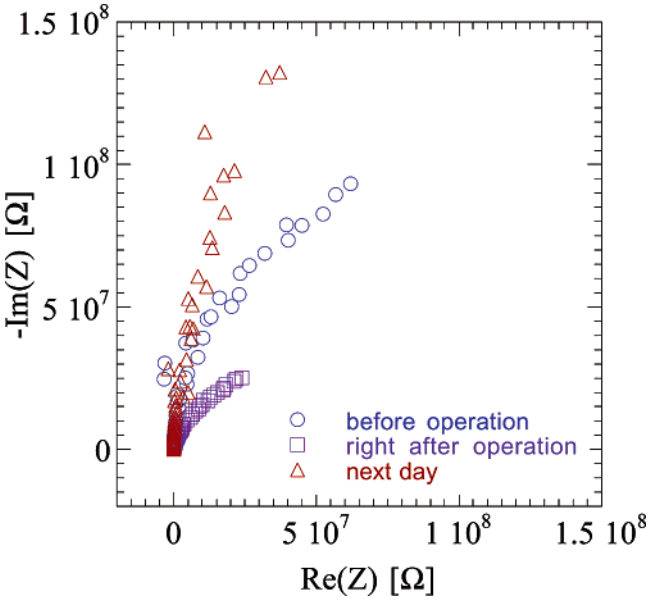

Figure 10. Zero bias AC impedance spectra for carbon IDA with $Ru(bpy)_3(ClO_4)_2$ before, immediately after and on the next day after operation at 3.5 V for 10 min (20 mV amplitude, 65 kHz − 10 Hz). After the second measurement (taken after device operation) the cell was left short-circuited for 20 h.

The results presented above are not unique for C IDAs or for $Ru(bpy)_3(ClO_4)_2$ films. Analogous results were obtained for Au electrodes separated by a 2−10 μm gap and for $Ru(bpy)_3(BF_4)_2$ films. In all such experiments a greater EL intensity was observed near or on the negatively charged electrode, and the location where EL was observed later exhibited lower PL intensity. As for the sandwich LECs, sealing such devices with epoxy cement in the drybox led to a prominent increase of stability and EL intensity.

Proposed Mechanism for the Degradation of $Ru(bpy)_3^{2+}$ LECs. The results on the electrical and optical properties of $Ru(bpy)_3^{2+}$ LECs indicate that hole injection (or generation of $Ru(bpy)_3^{3+}$ species) does not lead to device degradation. Nevertheless, it is still unclear from the described experiments whether the degradation originates from $Ru(bpy)_3^{+}$, $Ru(bpy)_3^{2+*}$, or from both.

Because of the resemblance between the character of PL and EL decay (see above), we believe that the primary reason for the permanent $Ru(bpy)_3^{2+}$ LEC degradation is the generation of a quencher in the thin layer near the cathode (where EL is observed) from a side reaction of $Ru(bpy)_3^{2+*}$. Even if this process is not very efficient, the concentration of the quencher need not be large to show a significant effect since, during device operation, it is generated in a thin layer exactly where the excited state is formed.

A possible product of this side reaction is $Ru(bpy)_2(H_2O)_2^{2+}$ which is known to form as a result of photodecomposition of $Ru(bpy)_3^{2+}$ in aqueous solutions[43] or as an intermediate product of photosubstitution reactions of $Ru(bpy)_3^{2+}$.[44] Purposely adding small amounts (1−4%) of $Ru(bpy)_2(H_2O)_2^{2+}$ in sandwich LECs considerably decreases their quantum efficiency, indicating that it can act as a quencher in the solid state (Figure 11). The quantum efficiency at 2.3 V decreases by more than 2 orders

(42) The same processes (PL recovery near anodes and permanent drop of PL intensty near cathodes) are also observed if a planar LEC is left without short circuiting. However, in this case the processes go much more slowly.

(43) Vaidyalingam, A.; Dutta, P. K. *Anal. Chem.* **2000**, *72*, 5219−5224.
(44) Tachiyashiki, S.; Ikezawa, H.; Mizumachi, K. *Inorg. Chem.* **1994**, *33*, 623−625.

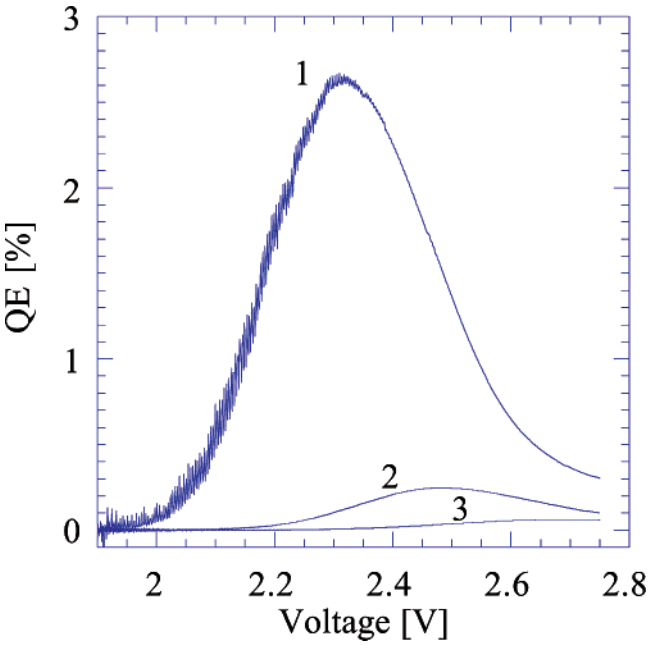

Figure 11. Quantum efficiency (QE) of ITO/$Ru(bpy)_3(ClO_4)_2$/Ga:In devices with various molar concentrations of $[Ru(bpy)_2(H_2O)_2](ClO_4)_2$: (1) 0%, (2) 1.44%, 3 (3).47%.

Table 1. Quantum Efficiency for ITO/$Ru(bpy)_3$/Ga−In Devices with Various Molar Concentrations of $[Ru(bpy)_2(H_2O)_2](ClO_4)_2$

$[Ru(bpy)_2(H_2O)_2](ClO_4)_2$ (% molar)	maximum quantum efficiency (%)	voltage at maximum quantum efficiency (V)	quantum efficiency at 2.3 V (%)
0	2−2.6	∼2.35	2.6
1.44	0.25	∼2.53	0.12
3.47	0.09	∼2.68	0.011

of magnitude for devices with 3.47% $[Ru(bpy)_2(H_2O)_2](ClO_4)_2$ (Table 1). The $[Ru(bpy)_2(H_2O)_2](ClO_4)_2$ complex oxidizes easily in air, and thus it may be the oxidation product which is responsible for EL quenching.

The presence of water molecules in this substance explains the much longer lifetime of the LEC as well as slower PL decay under drybox conditions where the water content is significantly lower than in air. One might note, however, that even under drybox conditions, some residual water that is retained in the original $Ru(bpy)_3X_2$ solution in acetonitrile can be present and might be critical to both cell operation and degradation.

The highly asymmetric injection into $Ru(bpy)_3^{2+}$ LEC causes EL to be generated in a thin layer near the cathode, so that degradation of a relatively small fraction of $Ru(bpy)_3^{2+}$ film causes a fast decay in device emission. As follows from the gradual shift of the EL maximum intensity toward the cathode, the carrier injection asymmetry is further increased during device operation, thereby accelerating EL decay. This suggests an explanation for the observed boost in the longevity of LECs operated under pulsed voltage.[29,31] EL decay is further accelerated by the decrease in device conductivity due to quencher formation as follows from the AC impedance study of the spent planar LEC (Figure 10) as well as from the darker EL observed for the preirradiated region of the sandwich LEC (Figure 5 c).

Conclusions

It is shown that the stability of tris(2,2′-bipyridine)ruthenium(II)-based light-emitting devices is greatly improved when they are produced and operated under drybox conditions. The proposed mechanism of the light-emitting device degradation involves formation of a quencher in a small fraction of tris(2,2′-bipyridine)ruthenium(II) film adjacent to the cathode, where light generation occurs. The formation of a quencher is also accompanied by an increase in device resistivity. Observed for the first time, the electroluminescence profile in tris(2,2′-bipyridine)ruthenium(II) devices constructed on interdigitated electrode arrays demonstrated that the charge injection in such devices is highly asymmetric because of more efficient hole injection. A microscopic study of photo- and electroluminescence profiles of planar light-emitting electrochemical cells was shown as a useful approach for studies of charge carrier injection into organic films.

Acknowledgment. Support by the Center for Nano- and Molecular Science and Technology, the Robert A. Welch Foundation, The National Science Foundation (CHE 0202136), and MURI (DAAD19-01-1-0676) is greatly appreciated. We thank Professor Milena Koudelka-Hep (Institute of Microtechnology, Neuchâtel, Switzerland) for providing C and Pt IDAs, and Dr. Donald Pile (The University of Texas at Austin) for useful discussions.

Supporting Information Available: Successive EL images of $Ru(bpy)_3(ClO_4)_2$ film spin-coated onto carbon IDA. Voltage: 7.5V and PL recovery in carbon IDA $Ru(bpy)_3(ClO_4)_2$ OLECs. This material is available free of charge via the Internet at http://pubs.acs.org

JA029550I